JJBS

Volume 17, Number 1,March 2024
ISSN 1995-6673
Pages 153 – 161
https://doi.org/10.54319/jjbs/170115

Jordan Journal of Biological Sciences

Potential Active Compounds of Propolis as Breast Anticancer Candidates: *In Silico* Study

Ruswanto Ruswanto[1], Tita Nofianti[1], Tresna Lestari[1], Ade Dwi Septian[1], Agung Purnama Firmansyah[2], Richa Mardianingrum[2,*]

[1]*Faculty of Pharmacy, Universitas Bakti Tunas Husada, Tasikmalaya, West Java, Indonesia;* [2]*Department of Pharmacy, Universitas Perjuangan, Tasikmalaya, West Java, Indonesia;*

Received: March 23, 2023; Revised: August 13, 2023; Accepted: August 26, 2023

Abstract

Breast cancer is the most common cancer in Indonesian women. A number of drugs derived from native ingredients have been widely developed and researched for the treatment of breast cancer, one of which is propolis from Indonesia. This study aims to determine the interaction of propolis bioactive compounds on the breast cancer receptor ERα and to establish its pharmacokinetic and toxicity properties *in silico.* The methods used include virtual screening toxicity, pharmacokinetics, docking, and molecular dynamic simulation of 111 bioactive compounds of propolis from was collected from database and compared with 4-hydroxytamoxifen (4-OHT). The results of virtual screening showed that propolis bioactive compounds had good pharmacokinetics, were not toxic and had the best Gibbs free energy (ΔG) and inhibition constant (Ki). Molecular dynamics simulations were continued for three compounds with the best virtual screening values, namely 4-OHT, PRO9 and PRO62. The conclusion of the molecular mechanics-Generalised Born surface area (MM-GBSA) calculation showed that PRO62 has the smallest ΔG_{total} value (-48.469 Kcal/mol) compared to 4-OHT and PRO9. The bioactive compound propolis, namely PRO62 or lanosterol (3-beta), has a more stable interaction than 4-OHT against ERα.

Keywords: anticancer, breast cancer, ERα, in silico, propolis

1. Introduction

Breast cancer is a type of cancer that occurs due to uncontrolled cell growth around the breast. According to statistical data released by the International Agency for Research on Cancer (IARC) in December 2020, the number of breast cancer cases has surpassed lung cancer as the most frequently diagnosed cancer in the world (World Health Organization, 2020). Of the 19.3 million new cancer cases, an estimated 2.3 million were new cases of breast cancer (11.7%), followed by lung cancer (11.4%), colorectal cancer (10.0%), prostate cancer (7.3%) and stomach cancer (5.6%) (Bray et al., 2018). Breast cancer is the most common type of cancer in Indonesian women, with 42.1 cases per 100,000 population and an average mortality rate of 17 per 100.000 population (Riskesdas, 2018). As many as 75% of cases are oestrogen receptor alpha breast cancer (Miah et al., 2019).

The high cost of cancer treatment and the ineffectiveness of treatment encourages people to choose treatment derived from native ingredients (Hasanah and Widowati, 2016). A number of drugs derived from native ingredients have been widely developed and researched for the treatment of breast cancer, one of which is propolis (Kustiawan et al., 2015). More than 300 compounds have been found in propolis scattered in various regions of the world. In general, the bioactive compounds of propolis are influenced by the bee species, the geographical origin of the beehive, and the source of the plant origin (Amalia et al., 2020).

Propolis from the tropics, especially in Southeast Asia, has become an interesting subject because it has various bioactive compounds that are not well known, but published data on propolis from Indonesia is very limited and has received little attention (Fikri et al., 2020). The propolis extract produced by *Trigona insica* bees from East Kalimantan had cytotoxic and apoptotic activity against cancer cells, with an IC_{50} value of 4.28±0.14 g/mL (Kustiawan et al., 2015). Another study conducted showed that propolis extract from Indonesia was able to inhibit the growth of MCF-7 cancer cells, with an IC_{50} value of 18.6±0.03 mg/mL (Amalia et al., 2020). Propolis originating from Indonesia is spread over several areas, including Java (Fikri et al., 2020), Sulawesi (Amalia et al., 2020; Miyata et al., 2019), Kalimantan (Kustiawan et al., 2015) and Sumatra (Kalsum et al., 2016).

In silico studies are widely used in drug research and development as a fast and inexpensive technique that can be applied in both academia and industry. This study aims to determine the interaction of propolis bioactive compounds on the breast cancer receptor ERα and to establish its pharmacokinetic and toxicity properties *in silico.*

* Corresponding author. e-mail: richamardianingrum@unper.ac.id.

2. Material and Methods

2.1. Materials

A personal computer with specification Intel(R) Core(TM) i5-8265U CPU @ 1.60GHz (8 CPUs) x 8.00 GB *of Ram 64-Bit Operating System of Windows 10* was used. The autodockTools 1.5.6 was used for preparation receptor and docking simulation, the *MarvinSketch* version 21.17.0 was used for preparation the compounds, *Discovery Studio Version* 20.1 was used for visualization 2D/3D, and *pkCSM* web-based programs for pharmacokinetics and toxicity prediction. The breast cancer receptor was downloaded from the PDB with codes 3ERT (https://www.rcsb.org/structure/3ERT).

2.2. Methods

2.2.1. Preparation of the structure of the Ligand

A total of 111 structures of propolis bioactive compounds (The detailed structures can be seen in Supplementary Table S1) and comparison compounds were collected and downloaded from database in http://pubchem.ncbi.nih.gov (Batra et al., 2022). Ligands were prepared using the *MarvinSketch 5.2.5.1* program; two-dimensional structural drawings were converted into three dimensions and then geometric estimation and ligand protonation at pH 7.4 were carried out, as well as a *conformational search*, which was subsequently saved in *.pdb* format (Ruswanto et al., 2023).

2.2.2. Receptor Analysis and Receptor Preparation

The receptors used were cancer receptors downloaded from the PDB on the http://rcsb.org/pdb website (Abuhamdah et al., 2020). Receptor analysis was performed at http://www.ebi.ac.uk/databases/cgi-bin/pdbsum/, with the requirement that the most favoured regions value > 90% and the disallowed regions value < 0.8% on the Ramachandran plot (Ho and Brasseur, 2005; Pratami et al., 2022). This was followed by protein preparations, which were carried out by removing water and charge on receptors with the help of the 2017 BIOVIA Discovery Studio program. Receptors and native ligand were stored in .pdb format.

Before the test ligand selection process was carried out in this study, receptor validation was first performed using the AutoDock 1.5.6 program (Al-Khayyat, 2021) by re-docking native ligands at the original receptor. The parameter used was RMSD (root mean square deviation), and the docking method was said to be valid if it had an RMSD value of ≤ 2Å (Bajda et al., 2014).

2.2.3. Molecular Docking & Virtual Screening Simulation

The study aimed to determine the best energy value (ΔG) and inhibition constant (Ki) of ligands as breast anticancer agents. Virtual screening was conducted with the PyRx 0.9.8 program on 111 test ligands and one comparison ligand. The results were visualized using BIOVIA Discovery Studio 2017 program, and the interaction between ligands and receptors was analysed using Discovery Studio software (Dallakyan and Olson, 2015; Tripathi et al., 2019).

2.2.4. Pharmacokinetics and Toxicity Prediction

The prediction of pharmacokinetic parameters (ADME) and toxicity was carried out with the help of pkCSM online tool. Compounds drawn using MarvinSketch 5.2.5.1 were converted into SMILES molecular format and then uploaded to http://biosig.unimelb.edu.au/pkcsm/prediction. The pharmacokinetic parameters used were Caco-2, human intestinal absorption (HIA), VDss, blood brain barrier (BBB) permeability, total clearance, and renal organic cation transporter 2 (OCT2) substrate. The toxicity parameters used were Ames toxicity, LD 50 and hepatotoxicity (Pires et al., 2015).

2.2.5. Molecular Dynamic Simulation

Simulations were carried out on test ligands that had the best value and compared using the *AMBER 16* program. The parameters used in the *molecular dynamics* were *root mean square fluctuation (RMSF), RMSD* and *molecular mechanics-Generalised Born surface area* (*MM-GBSA).*(Mardianingrum et al., 2020) The simulation was carried out with several stages, namely parameterisation, system minimisation, equilibration, *heating* and production (Mardianingrum et al., 2022) .

3. Results

3.1. Receptor Analysis and Preparation

The receptor used was the breast cancer receptor (ERα) with PDB code 3ERT (Shiau et al., 1998). The receptor was downloaded from the site http://rcsb.org/pdb. The x-ray diffraction protein crystal structure was obtained from the human oestrogen receptor with a resolution of 1.90. This receptor has the native ligand 4-hydroxytamoxifen (4-OHT) bound to 247 amino acid residues. Receptor analysis was carried out by looking at the statistics of the Ramachandran plot via the website http://www.ebi.ac.uk/pdbsum. This Ramachandran plot was used to see the stability and quality of the protein, with the requirements for the most favoured regions > 90% indicated by the red area, and the disallowed regions < 0.8% value indicated by the white area (Ho and Brasseur, 2005). Based on the results of the 3ERT receptor analysis, the number of amino acids distributed in the most favoured regions is 91.2%, and the amino acids in the disallowed regions are 0.0%; so, it can be stated that the protein structure of the 3ERT receptor is stable and has met the requirements. The structure of the 3ERT receptor protein and Ramachandran plot can be seen in Figure 1.

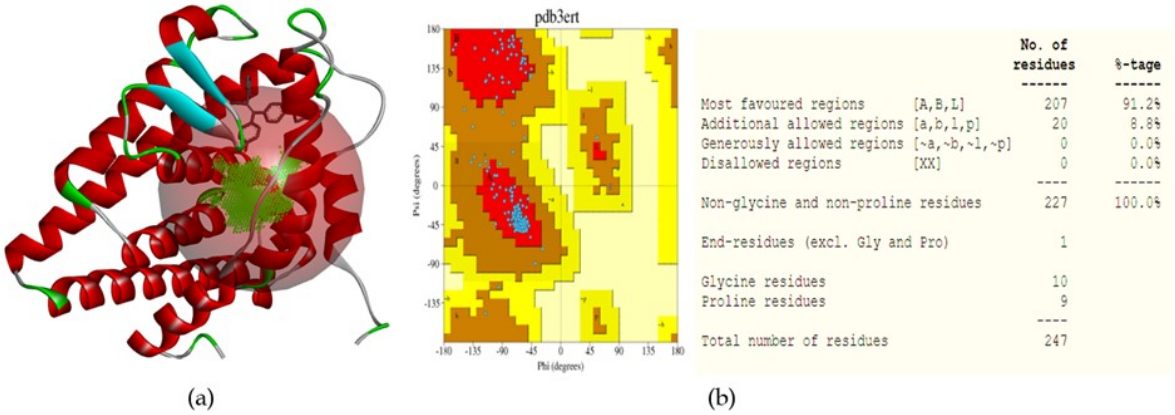

Figure 1. The structure of the 3ERT receptor protein (a) and Ramachandran plot (b).

3.2. Validation Docking

Receptor validation or re-docking was carried out by docking native ligand (4-OHT) to the prepared receptor using the AutoDock 1.5.6 program. The RMSD value is used as a parameter to determine the accuracy of the docking method. A small RMSD value indicates that the conformation of the ligand is close to the original position before re-docking; this value can be obtained by adjusting the coordinates of the grid box (x, y, z) where the interaction between the receptor and the ligand occurs. The Lamarckian Genetic Algorithm calculation system was chosen, with GA_run 100. The docking validation method was said to be valid if it had an RMSD value of 2Å (Bajda et al., 2014; Ruswanto et al., 2020). The overlay of native ligand poses with re-docked ligands and the position of the ligands in the grid box can be seen in Figure 2.

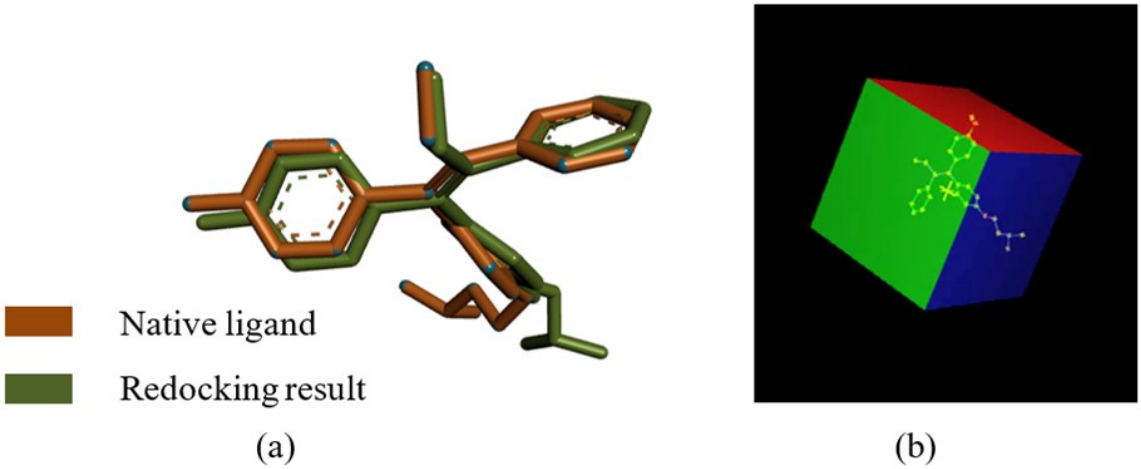

Figure 2. Overlay native ligand pose (4-OHT) crystallographic results with re-docking results (a) and ligand position in grid box (b).

Table 1 Docking Method Validation Results

Protein Data Bank (PDB) Code	*Centre Grid Box*	*Box Dimension*	*Space*	RMSD (Å)	*Binding Affinity* (kcal/mol)
3ERT	x = 30.191 y = -1.913 z = 24.207	x = 40 y = 40 z = 40	0.375	1.09	-11.52

Based on Table 1, the docking validation can be said to meet the requirements, with an RMSD value of 1.09Å, so the grid box coordinates (x, y, z) and box dimensions can be used as a reference for conducting a virtual screening process using the PyRx 9.8 program.

3.3. Simulation Molecular Docking & Virtual Screening

Virtual screening was conducted to select propolis bioactive compounds that have the most stable interaction with the 3ERT receptor in terms of binding energy (ΔG) and inhibition constant (Ki) values using the PyRx 0.9.8 program. A total of 111 structures of propolis bioactive compounds were downloaded from http://pubchem.ncbi.nih.gov, and the ligands were then screened by activating the docking menu in the PyRx 0.9.8 program. The comparison compound used was 4-OHT, which also acts as a native ligand found in the 3ERT receptor. The coordinates of the grid box from the validation of the docking method (Table 1) were used as a reference for screening. The results of virtual screening can be seen in Table 2.

The structure of the three compounds with the best virtual screening values can be seen in Figure 3.

Table 2 Virtual screening results of ligands with the best binding affinities

Code	Compound	ΔG (Kcal/mol)	Ki (μM)
4-OHT	4-hydroxytamoxifen (native ligand)	-11.21	0.006
PRO9	7-{2-[(2E)-3,7-dimethylocta-2,6-dien-1-yl]-3,4-dihydroxyphenyl}-4-hydroxy-3-(3-methylbut-2-en-1-yl)-5-oxo-5,6,7,8-tetrahydronaphthalen-2-olate	-10.73	0.013
PRO62	(1S,2R,5S,10R,11S,14R,15R)-2,6,6,11,15-pentamethyl-14-[(2R)-6-methylheptan-2-yl]tetracyclo[8.7.0.0^{2,7}.0^{11,15}]heptadec-7-en-5-ol	-10.42	0.022
PRO61	(1S,2R,5R,10R,11S,14R,15R)-2,6,6,11,15-pentamethyl-14-[(2R)-6-methylheptan-2-yl]tetracyclo[8.7.0.0^{2,7}.0^{11,15}]heptadec-7-en-5-ol	-10.29	0.028
PRO64	(2S,5S,7R,11S,14S,15S)-2,6,6,11,15-pentamethyl-14-[(2S)-6-methylhept-5-en-2-yl]tetracyclo[8.7.0.0^{2,7}.0^{11,15}]heptadec-1(10)-en-5-ol	-10.15	0.036
PRO63	(1S,2R,10R,11S,14R,15R)-2,6,6,11,15-pentamethyl-14-[(2R)-6-methylheptan-2-yl]tetracyclo[8.7.0.0^{2,7}.0^{11,15}]heptadec-7-en-5-yl acetate	-9.95	0.050
PRO67	(1S,3R,6S,8R,12S,15R,16R)-7,7,12,16-tetramethyl-15-[(2R)-6-methyl-5-methylideneheptan-2-yl]pentacyclo[9.7.0.0^{1,3}.0^{3,8}.0^{12,16}]octadecan-6-ol	-9.82	0.063
PRO6	3-{2-[(2E)-3,7-dimethylocta-2,6-dien-1-yl]-3,4-dihydroxyphenyl}-6,8-dihydroxy-1,2,3,4-tetrahydronaphthalen-1-one	-9.75	0.082
PRO8	3-{3-[(3E)-4,8-dimethylnona-3,7-dien-1-yl]-4,5-dihydroxyphenyl}-6,8-dihydroxy-1,2,3,4-tetrahydronaphthalen-1-one	-9.55	0.099
PRO66	(3S,6aR,6bS,8aR,12aS,14bR)-4,4,6a,6b,8a,11,11,14b-octamethyl-1,2,3,4,4a,5,6,6a,6b,7,8,8a,9,10,11,12,12a,14,14a,14b-icosahydropicen-3-yl acetate	-9.32	0.148
PRO83	6-{6-hydroxy-7,7,12,16-tetramethylpentacyclo[9.7.0.0^{1,3}.0^{3,8}.0^{12,16}] octadecan-15-yl}-2-methyl-3-methylideneheptanoate	-9.13	0.202
PRO47	(1R,2S,5R,8S,9S,10S,13R,14R,17S,19R)-1,2,5,9,10,14,18,18-octamethyl-8-(prop-1-en-2-yl)pentacyclo[11.8.0.0^{2,10}.0^{5,9}.0^{14,19}]henico san-17-o	-8.82	0.340
PRO82	2-methyl-3-methylidene-6-{7,7,12,16-tetramethyl-6-oxopentacyclo[9.7.0.0^{1,3}.0^{3,8}.0^{12,16}]octadecan-15-yl}heptanoate	-8.64	0.462
PRO7	3-(3,4-dihydroxyphenyl)-7-[(3E)-4,8-dimethylnona-3,7-dien-1-yl]-6,8-dihydroxy-1,2,3,4-tetrahydronaphthalen-1-one	-8.63	0.475
PRO78	5-hydroxy-2-(4-hydroxyphenyl)-8-(3-methylbut-2-en-1-yl)-4-oxo-4H-chromene-3,7-bis(olate)	-8.59	0.501
PRO21	1-(3-cyclohexyl-3-hydroxy-3-phenylpropyl)piperidin-1-ium	-8.31	0.810
PRO85	(1S,3R,6S,8R,11S,12S,15R,16R)-15-[(2R,5Z)-hept-5-en-2-yl]-7,7,12,16-tetramethylpentacyclo[9.7.0.0^{1,3}.0^{3,8}.0^{12,16}] octadecan-6-ol	-8.3	0.828
PRO69	(11S,15S,16R)-2-methoxy-16-(7-methoxy-2H-1,3-benzodioxol-5-yl)-4,6,13-trioxatetracyclo[7.7.0.0^{3,7}.0^{11,15}]hexadeca- 1(9),2,7-triene	-8.09	1.18
PRO68	(3S,4aR,6aR,6bS,8aR,11R,12S,12aR,14aR,14bR)-4,4,6a,6b,8a,11,12,14b-octamethyl-1,2,3,4,4a,5,6,6a,6b,7,8,8a,9,10,11,12,12a,14,14a,14b-icosahydropicen-3-yl acetate	-7.96	1.46
PRO77	5,7,8-trihydroxy-2-[4-hydroxy-3-(3-methylbut-2-en-1-yl)phenyl]-6-(3-methylbut-2-en-1-yl)-4-oxo-4H-chromen-3-olate	-7.89	1.65
PRO48	(4aS,6aS,8aS,9R,12bR,14aR)-2,2,4a,6a,8a,9,12b,14a-octamethyl-docosahydropicene	-7.88	1.67

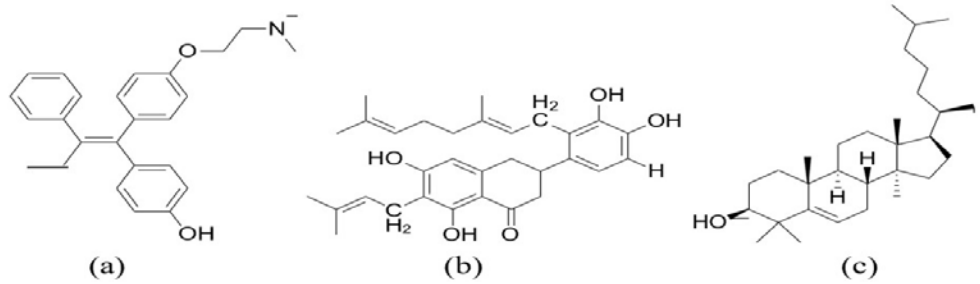

Figure 3. The structure of the compounds having the best virtual screening value 4-OHT (a), PRO9 (b), PRO63 (c).

3.4. Docking Result Visualisation Analysis

The BIOVIA Discovery Studio 2017 program was used to visualize the interaction between ligands and amino acid residues from the 3ERT receptor. The structure of an amino acid consists of a C atom covalently bonded to a carboxyl group, amine group, H atom, and side chain or R group. Hydrogen bonding is an important bond between the ligand and the receptor, affecting the molecule's affinity to the target protein. Hydrophobic bonds, non-covalent bonds, determine the ligand's stability with the

target protein, forming groups on the polar side of the protein structure due to the merging of non-polar chains (Harti, 2014); (Herschlag and Pinney, 2018; Siswandono, 2020); (Gouda and Almalki, 2019). The docking interaction results can be seen in Table 3.

Table 3 Interaction with amino acids

No.	Compound	Bond Type			
		Hydrogen	Pi-sigma Pi-sulphur Amide	Pi-alkyl/alkyl	van der Waals
1	4-OHT	Glu353, Arg394	-	Ala350, Leu387, Leu391, Phe404, Met421, Leu428, Leu525	Met343, Leu346, Thr347, Leu349, Asp351, Glu353, Leu354, Trp383, Leu384, Met388, Glu419, Gly420, Ile424, Gly521, His524, Met528, Leu536
2	PRO9	Leu387, Arg394, Met343	Met343, Leu346, Leu525	Ala350, Leu391, Phe404, Met421, Leu428, His524, Met528	Thr347, Leu349, Glu353, Trp383, Met388, Gly420, Ile424, Gly521, Lys529
3	PRO62	Asp351	-	Leu346, Leu349, Ala350, Leu384, Leu387, Leu391, Phe404, Leu525	Met343, Thr347, Glu353, Met388, Arg394, Met528

From the binding site prediction, it can be seen that the amino acids present in the binding site area are Met342, Leu345, Leu346, Leu349, Asp351, Arg352, Ala382, Trp383, Ile 386, Leu403, Val418, Glue419, Gly420, Met427, Lys520 and His524. And it can be seen that there are amino acids in the binding site area of 3ERT that interact with ligands, for example the PRO9 compound (Leu346, His524, Leu349, Trp383 dan Gly420). Visualisation of the interaction of the ligand to the 3ERT receptor can be seen in Figure 4.

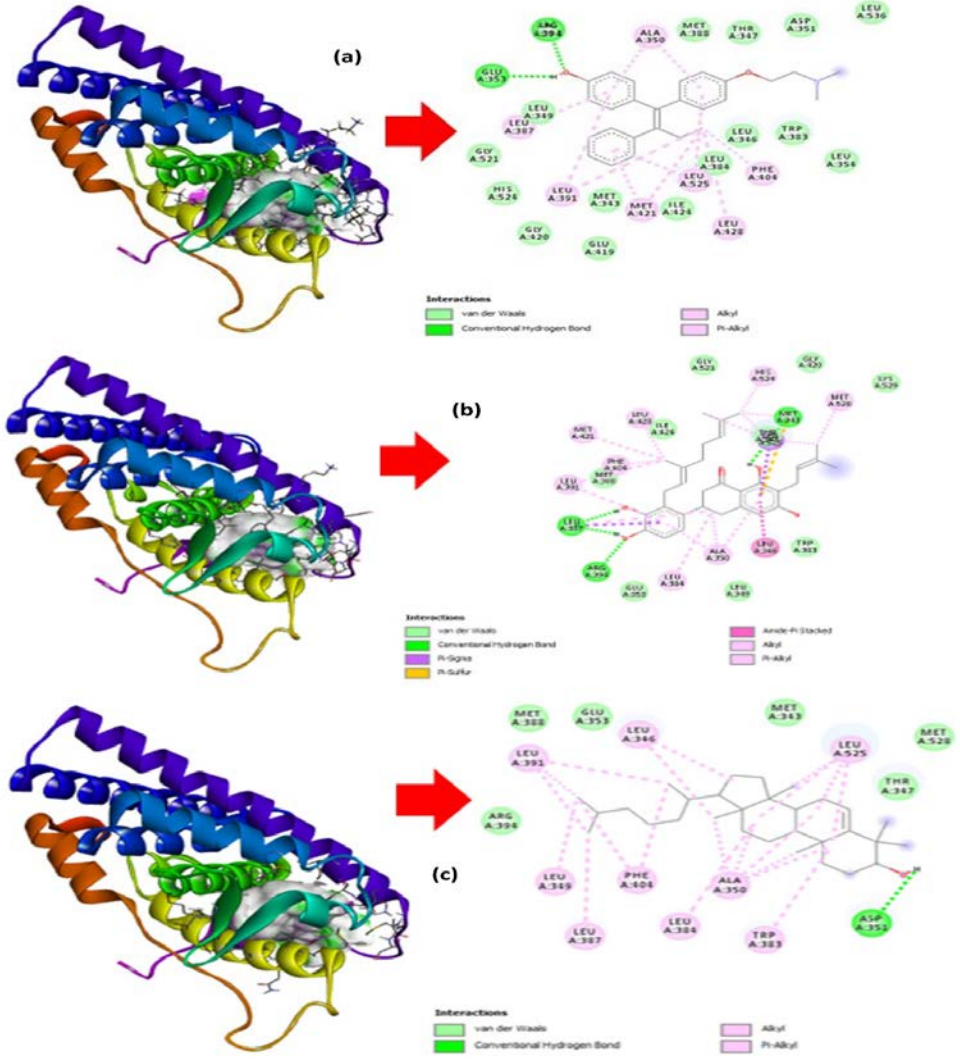

Figure 4. The 2D and 3D visualisation of the interaction of the ligand to the 3ERT receptor (a) native.

3.5.

3.6. Pharmacokinetics and Toxicity Prediction

Two propolis bioactive compounds and a comparison compound (4-OHT) with the best virtual screening values were selected to predict pharmacokinetic and toxicological properties. The pharmacokinetic parameters used were the Caco-2, HIA, VDss, BBB permeability, total clearance and renal OCT2 substrate, while the toxicity parameters used were Ames toxicity, LD 50 and hepatotoxicity (Pires et al., 2015). The Pharmacokinetic result can be seen in Table 4.

Table 4 Pharmacokinetics Parameters

		Pharmacokinetics Parameters					
		Absorption		Distribution	Metabolism	Excretion	
No	Compounds	Caco-2 (Log cm/s)	HIA (%)	VDss (Log L/Kg)	BBB (Log BB)	CYP3A4 Substrate	Renal OCT2 substrate
1	4-OHT	1.120	95.378	0.156	-0.288	Yes	No
2	PRO9	0.941	86.731	-0.165	-1.091	Yes	No
3	PRO62	1.284	97.308	0.196	0.769	Yes	No

Note: HIA – human intestinal absorbance; BBB – blood brain barrier.

Based on Table 4, the CaCo-2 is used to predict the permeability of drug compounds. A drug is said to have high permeability if the CaCo-2 value is > 0.90 Log cm/s (Pires et al., 2015). Based on Table 4, several compounds met the requirements. HIA is used to predict drug absorption in the intestine. A drug has good absorption if it has an HIA value > 80% and poor absorption if the HIA value is < 30% (Chander et al., 2017). Based on the data from Table 4, propolis bioactive compounds and comparison compounds had good absorption (> 80%).

VDss is used to predict the drug concentration in blood plasma. The higher the VDss value, the higher the drug distribution to the tissues (Pires et al., 2015). The VDss value is said to be low if < -0.5 and high if > 0.45. Based on Table 4, several compounds had good drug distribution values.

BBB permeability is used to predict the ability of drugs to penetrate the blood brain barrier. This parameter is important to reduce the toxic effects and side effects of a drug. A BBB value > 0.3 is estimated to be able to penetrate the blood brain barrier well, while a BBB value < -1 is estimated to have a poor ability to penetrate the blood brain barrier (Pires et al., 2015). Based on Table 4, several compounds have good BBB values and can be predicted to have few side effects and low toxicity.

CYP3A4 substrate is used to predict drug metabolism, which generally occurs in the liver by involving brain cytochrome P450 enzymes (Pires et al., 2015). Based on Table 4, most of the compounds were metabolised by cytochrome P450 enzymes. OCT2 was used to predict drug excretion. The substrate of OCT2 has the potential to cause side interactions. Based on Table 4, several compounds are not substrates of OCT2.

Table 5 The Toxicity Parameters

		Toxicity Parameters		
No	Compounds	Ames Toxicity	LD 50 (mol/kg)	Hepatotoxicity (Yes/No)
1	4-OHT	Yes	2.069	No
2	PRO9	No	2.144	No
3	PRO62	No	3.598	No

The toxicity parameters are given in Table 5. Ames toxicity was used to predict the mutagenic potential of the compound. Positive test results indicate the ability of the compound to act as a carcinogen (Pires et al., 2015). The mutagenic ability of 4-OHT is in line with the theory that the use of tamoxifen has the potential to cause uterine cancer (Lorizio et al., 2012). The LD50 was used as a reference standard for acute toxicity measurements.

3.7. Molecular Dynamics

Molecular dynamic simulations were conducted using the AMBER 16 program to analyze the interaction, flexibility, and stability of propolis bioactive compounds, such as PRO9 and PRO62, compared to 4-OHT. The simulation involved preparing receptors and ligands, parameterizing the system, and constructing complex topology coordinates. The general amber force field (GAFF) was used to construct the topology on the ligands, and the ff14SB force field was used for the protein. The system was neutralized by adding Na+ ions or Cl- ions, and energy minimisation was performed. The system was heated at 0-310 K, and equilibration was performed six times to maintain constant volume, pressure, and temperature. The final stage involved production for 20 ns. The RMSD value was used to determine molecular conformation shifts, with stable values up to 0.1 nm indicating protein stability (Desheng et al., 2011; Muttaqin, 2019).

The RMSD graph of the 4-OHT, PRO9 and PRO62 systems can be seen in Figure 5.

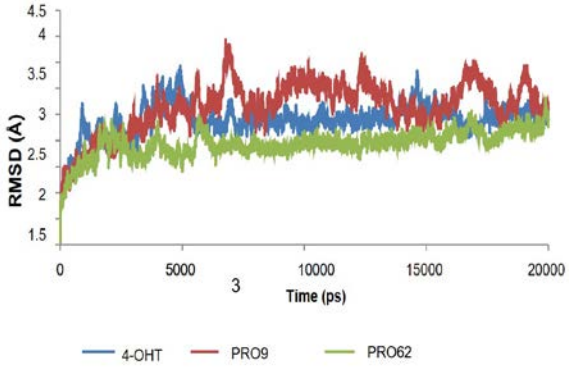

Figure 5. The RMSD for 4-OHT, PRO9 and PRO62

RMSF is used to see fluctuations in the shift of amino acid residues that make up proteins that interact with ligands. The RMSF value shows the size of the deviation between the particle position and several reference positions to describe the conformational shift of each amino acid residue that gives flexibility to the protein. The RMSF graph of the 4-OHT, PRO9 and PRO62 systems against the 3ERT receptor can be seen in Figure 6.

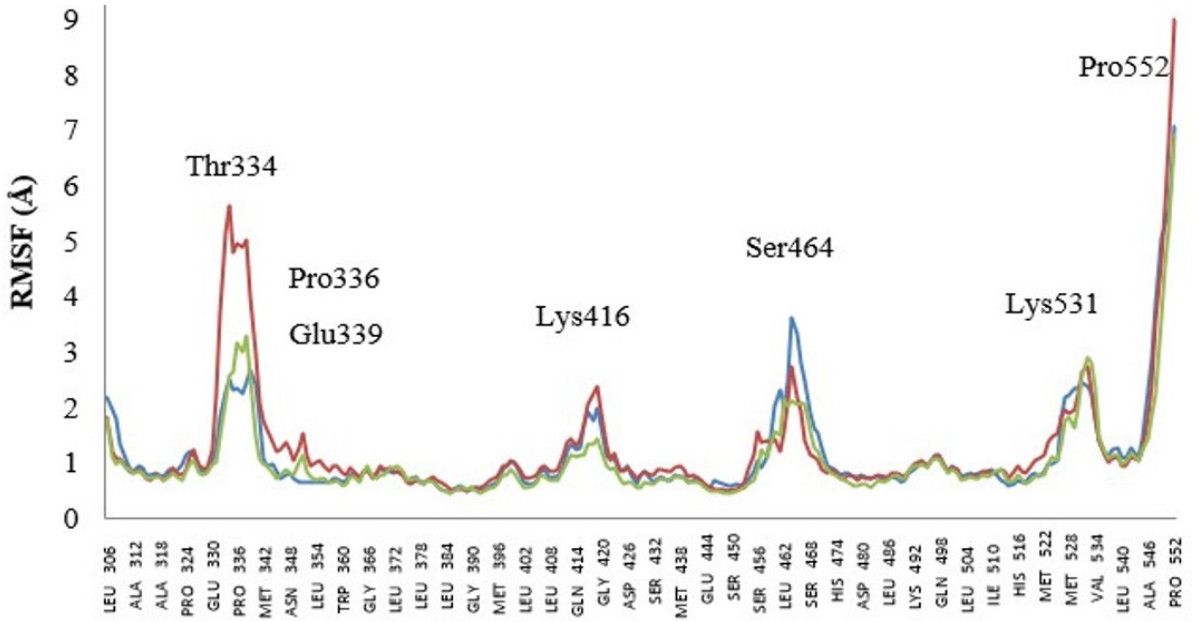

Figure 6. The RMSF for 4-OHT, PRO9 and PRO62.

The MM-GBSA was used to calculate the total bond energy (ΔG_{Total}) that occurred in the ligand-receptor system during the simulation. The smaller the value of free energy (ΔG) is, the more stable the interaction produced by the ligand-receptor system will be. The MMGBSA results can be seen in Table 6.

Table 6 Values of Molecular Mechanics-Generalised Born Surface Area (MM-GBSA) System 4-OHT, PRO9 and PRO62 against 3ERT

Parameters (Kcal/mol)	System		
	4-OHT	PRO9	PRO62
Interaction van der Waals (vdW)	-49.450	-47.141	-41.225
Electrostatic Energy (EEL)	111.070	125.898	87.489
Electrostatic contribution to solvation free energy (EGB)	-90.978	-103.303	-88.822
Non-polar contribution to solvation free energy (ESURF)	-7.169	-65.389	-5.912
ΔG_{Gas} (vdW+ EEL)	61.621	78.757	46.265
ΔG_{Solv} (EGB+ ESURF)	-98.147	-109.842	-9.473
ΔG_{Total} (vdW+EEL+EGB+ SURF)	-36.527	-31.085	-48.469

4. Discussion

Based on Table 2, the 20 compounds with the best virtual screening values were selected from 111 bioactive compounds of propolis. The Gibbs free energy (ΔG) was used to measure the ability of the ligand to bind to the receptor, while the value of the inhibitory constant (Ki) was used to measure the inhibitory activity. The smaller the ΔG value is, the higher are the bond affinity and the inhibitory activity, and the smaller is the Ki value, so that the ligands can form stronger and more stable bonds (Mardianingrum et al., 2021). It is known that the compounds with the best ΔG and Ki values, respectively, are 4-OHT (-11.21 Kcal/mol; 0.06 M), PRO9 (-10.73 Kcal/mol; 0.013 M) and PRO62 (-10.42 Kcal/mol; 0.022 M), so it can be said that the comparison compound 4-OHT has the most stable binding to the ERα receptor.

Based on Table 3, it can be seen that the 4-OHT compound has two hydrogen bonds to Glu353 and Arg394, while PRO9 has three hydrogen bonds to Met343, Leu387, Arg394, and PRO62 has one hydrogen bond with the Asp351 residue. PRO9 has a hydrogen bond equation with 4-OHT bonded to Arg394, which indicates a similarity in forming a stable bond with ERα. The ERα has hydrogen bonds with amino acid residues of His524, so the ligand can be an agonist if it has hydrogen bonds with His524, which causes helix-12 to open (Muchtaridi et al., 2014). Based on Table 3, 4-OHT, PRO9 and PRO62 do not have hydrogen bonds with His524, so they are predicted to have antagonistic properties that can block the binding of coactivators to the ERα receptor.

4-OHT has 17 hydrophobic bonds with Met343, Leu346, Thr347, Leu349, Asp351, Glu353, Leu354, Trp383, Leu384, Met388, Glu419, Gly420, Ile424, Gly521, His524, Met528 and Leu536. PRO9 has 13 hydrophobic bonds with 4-OHT, namely Thr347, Leu349, Ala350, Glu353, Trp383, Met388, Leu391, Phe404, Gly420, Met421, Ile424, Leu428 and Gly521, while PRO62 has the same 10 hydrophobic bonds: Met343, Thr34, Ala350, Glu353, Leu387, Met388, Leu391, Phe404, Leu525 and Met528. The existence of a hydrophobic bond equation indicates the similarity of the drug's ability to penetrate biological membranes so that it is predicted to bind well to Erα, and the number of pi-sigma interactions (pi-alkyl and pi-sulphur), which mostly involve charge transfer, helps in the drug interactions at the receptor binding site (Gouda and Almalki, 2019).

From the matching interaction of amino acid residues of PRO9 and PRO62 with the comparison compound (4-OHT), it can be predicted that both compounds have the same activity, and the number of interactions with amino acid residues can affect the bond energy that occurs between the ligand and the 3ERT receptor.

Based on Figure 5, it can be seen that there was an increase in the RMSD value during the molecular dynamic simulation, indicating that the ligand was ready to form bonds with the open protein structure. The highest RMSD value of the comparison compound 4-OHT was ± 3.5 at 5

ns, whilst the highest RMSD values of PRO9 and PRO62 were ± 4 at 7 ns and ± 2.5 at 19 ns, respectively. In this study, it can be seen that the PRO62 system can maintain its structure until the simulation ends and has a good level of stability compared to 4-OHT and PRO9; it can therefore be predicted to have a stable interaction with the 3ERT receptor, but all systems had not reached a completely stable conformation at the end of the simulations, so additional simulation time is needed.

Based on Figure 6, it can be seen that the RMSF value of the system is determined by fluctuations that occur in the amino acid residues. The highest fluctuation in the 4-OHT system occurred in Pro552, Lys531, Ser464, Lys416 and Glu334, while the residues that experienced the lowest fluctuations were Glu385, Ile389 and Leu384. The highest fluctuations in the PRO9 system occurred in Pro552, Thr334, Lys416, Ser464 and Lys531, while the residues that experienced the lowest fluctuations were Glu385, Ile389 and Leu384. The highest fluctuations in the PRO62 system occurred in Pro552, Lys531, Ser464 and Pro336, while the residues that experienced the lowest fluctuations were Glu385, Ile389 and Leu384.

The protein structure of ERα has hydrogen bonds attached to amino acid residues formed between Glu19 and His52, and between Glu19 and Lys531. Thus, if there is a significant fluctuation in the amino acid residue, the ligand can be predicted to have antagonistic properties to Erα.(Muchtaridi et al., 2014) The three systems, 4-OHT, PRO9 and PRO62, had increased fluctuations in lys531, which disrupted the hydrogen bonding of ERα so that 4-OHT, PRO9 and PRO62 could all be predicted to have potential as antagonists to ER.

Based on Table 6, it can be seen that the PRO62 system has the smallest ΔG_{Total} (-48.469 Kcal/mol) compared to 4-OHT (-36.527 Kcal/mol) and PRO9 (-31.085 Kcal/mol). Electrostatic energy has a great influence on the system. This shows that the PRO62 compound has a better affinity for the ERα breast cancer receptor (3ERT), so the compound can be predicted to have better potential as a breast cancer drug than the 4-OHT comparison drug by forming a more stable bond. The results of this study are also directly equivalent to several studies that reveal that lanosterol compounds have the potential to be developed as anticancer drugs.(Lasunción et al., 2012; Chung et al., 2010; Sanora et al., 2019).

5. Conclusion

A bioactive compound of propolis from was collected from database, namely PRO62 or lanosterol (3-beta) from Java and Kalimantan, has a more stable interaction than tamoxifen on breast cancer receptors (ERα), with a ΔG_{Total} value of -48.469 Kcal/mol. This compound met the pharmacokinetic requirements and had lower toxicity than tamoxifen.

Acknowledgments

The authors thank Universitas Bakti Tunas Husada and Universitas Perjuangan for the equipment provided for the research.

Disclosure

The authors report no conflicts of interest in this work.

References

Abuhamdah S, Abuhamdah R, Howes M J and Chazot P L. 2020. A Molecular Docking Study of Aloysia citrodora Palau. Leaf Essential Oil Constituents towards Human Acetylcholinesterase: Implications for Alzheimer's disease. *Jordan J Biol Sci*., **13(Supp. Issue)**: 575–580.

Al-Khayyat M Z. 2021. In Silico Screening for Inhibitors Targeting 4-diphosphocytidyl-2-C-methyl-D-erythritol Kinase in Salmonella typhimurium. *Jordan J. Biol. Sci*., **14(1)**: 75–82. https://doi.org/10.54319/140110.

Amalia E, Diantini A and Subarnas A. 2020. Water-soluble propolis and bee pollen of Trigona spp. from South Sulawesi Indonesia induce apoptosis in the human breast cancer MCF-7 cell line. *Oncol. Lett*., **20(5)**: 1–1. https://doi.org/10.3892/ol.2020.12137.

Bajda M, Jończyk J, Malawska B and Filipek S. 2014. Application of Computational Methods for the Design of BACE-1 Inhibitors: Validation of in Silico Modelling. *Int. J. Mol. Sci*., **15(3)**: 5128–5139. https://doi.org/10.3390/ijms15035128.

Batra B, Sudan S S, Pant M, Pant K, Lal A and Gusain T. 2022. Molecular docking and TLC analysis of candidate compounds from lesser used medicinal plants against diabetes mellitus targets. *Jordan J. Biol. Sci*., **15(2)**: 339–346. https://doi.org/10.54319/jjbs/150221.

Bray F, Ferlay J, Soerjomataram I, Siegel R L, Torre L A and Jemal A. 2018. Global cancer statistics 2018: GLOBOCAN estimates of incidence and mortality worldwide for 36 cancers in 185 countries. *CA. Cancer J. Clin*., **68(6)**: 394–424. https://doi.org/10.3322/caac.21492.

Chander S, Tang C R, Al-Maqtari H M, Jamalis J, Penta A, Hadda T B, Sirat H M, Zheng Y T and Sankaranarayanan M. 2017. Synthesis and study of anti-HIV-1 RT activity of 5-benzoyl-4-methyl-1,3,4,5-tetrahydro- 2H -1,5-benzodiazepin-2-one derivatives. *Bioorganic Chem*., **72(6)**: 74–79. https://doi.org/10.1016/j.bioorg.2017.03.013.

Chung M J, Chung C K, Jeong Y and Ham S S. 2010. Anticancer activity of subfractions containing pure compounds of chaga mushroom (Inonotus obliquus) extract in human cancer cells and in balbc/c mice bearing sarcoma-180 cells. *Nutr Res Pract*., **4(3)**: 177-182. https://doi.org/10.4162/nrp.2010.4.3.177.

Dallakyan S and Olson AJ. 2015. Small-Molecule Library Screening by Docking with PyRx, in: Hempel JE, Williams CH and Hong CC (Eds), **Methods in Molecular Biology**. Springer New York, New York, pp. 243–250. https://doi.org/10.1007/978-1-4939-2269-7_19.

Desheng L, Jian G, Yuanhua C, Wei C, Huai Z and Mingjuan J. 2011. Molecular dynamics simulations and MM/GBSA methods to investigate binding mechanisms of aminomethylpyrimidine inhibitors with DPP-IV. Bioorg. Med. Chem. Lett., **21(22)**: 6630–6635. https://doi.org/10.1016/j.bmcl.2011.09.093.

Fikri A M, Popova M, Sulaeman A and Bankova V. 2020. Stingless bees and Mangifera indica: A close relationship? Indian J. Nat. Prod. Resour., **11(2)**: 130–134. https://doi.org/10.56042/ijnpr.v11i2.25682.

Gouda A M and Almalki F A. 2019. Carprofen: a theoretical mechanistic study to investigate the impact of hydrophobic interactions of alkyl groups on modulation of COX-1/2 binding selectivity. *SN Appl. Sci*., **1(4)**: 332. https://doi.org/10.1007/s42452-019-0335-5.

Harti. 2014. **Health Biochemistry (Biokimia Kesehatan)**, Nuha Medika, Yogyakarta.

Hasanah S N and Widowati L. 2016. Jamu in tumor/cancer patients as complementary therapy. *J. Kefarmasian Indones*., **6(1)**: 49–59. https://doi.org/10.22435/jki.v6i1.5469.49-59.

Herschlag D and Pinney M M. 2018. Hydrogen bonds: simple after all? *Biochemistry*., **57(24)**: 3338–3352. https://doi.org/10.1021/acs.biochem.8b00217.

Ho B K and Brasseur R. 2005. The Ramachandran plots of glycine and pre-proline. *BMC Struct. Biol*., **5(1)**: 14. https://doi.org/10.1186/1472-6807-5-14.

Kalsum N, Setiawan B and Wirawati C U. 2016. Phytochemical studies and GC-MS analysis of propolis trigona spp. from two region in Lampung Province of Indonesia. Int. J. Sci. Eng. Res., **7(10)**: 173–180.

Kustiawan P M, Phuwapraisirisan P, Puthong S, Palaga T, Arung E T and Chanchao C. 2015. Propolis from the stingless bee trigona incisa from East Kalimantan, Indonesia, induces in vitro cytotoxicity and apoptosis in cancer cell lines. *Asian Pac. J. Cancer Prev*., **16(15)**: 6581–6589. https://doi.org/10.7314/APJCP.2015.16.15.6581.

Lasunción M A, Martín-Sánchez C, Canfrán-Duque A and Busto R. 2012. Post-lanosterol biosynthesis of cholesterol and cancer. *Curr. Opin. Pharmacol*., **12(6)**: 717–723. https://doi.org/10.1016/j.coph.2012.07.001.

Lorizio W, Wu A H B, Beattie M S, Rugo H, Tchu S, Kerlikowske K and Ziv E. 2012. Clinical and biomarker predictors of side effects from tamoxifen. Breast Cancer Res. Treat., **132(3)**: 1107–1118. https://doi.org/10.1007/s10549-011-1893-4.

Mardianingrum R, Endah S R N, Suhardiana E, Ruswanto R and Siswandono S. 2021. Docking and molecular dynamic study of isoniazid derivatives as anti-tuberculosis drug candidate. *Chem. Data Collect*., **32(4)**: 100647. https://doi.org/10.1016/j.cdc.2021.100647.

Mardianingrum R, Hariono M, Ruswanto R, Yusuf M and Muchtaridi M. 2022. Synthesis, Anticancer Activity, Structure–Activity Relationship, and Molecular Modeling Studies of α-Mangostin Derivatives as hERα Inhibitor. *J. Chem. Inf. Model*., **62(21)**: 5305–5316. https://doi.org/10.1021/acs.jcim.1c00926.

Mardianingrum R, Yusuf M, Hariono M, Mohd Gazzali A and Muchtaridi M. 2020. α-Mangostin and its derivatives against estrogen receptor alpha. *J. Biomol. Struct. Dyn*., **40(6)**: 2621-2634. https://doi.org/10.1080/07391102.2020.1841031.

Miah S, Bagu E, Goel R, Ogunbolude Y, Dai C, Ward A, Vizeacoumar F S, Davies G, Vizeacoumar F J, Anderson D and Lukong K E. 2019. Estrogen receptor signaling regulates the expression of the breast tumor kinase in breast cancer cells. *BMC Cancer*., **19(1)**: 78. https://doi.org/10.1186/s12885-018-5186-8

Miyata R, Sahlan M, Ishikawa Y, Hashimoto H, Honda S and Kumazawa S. 2019. Propolis components from stingless bees collected on South Sulawesi, Indonesia, and their xanthine oxidase inhibitory activity. *J. Nat. Prod*., **82(2)**: 205–210. https://doi.org/10.1021/acs.jnatprod.8b00541.

Muchtaridi M, Yusuf M. Diantini A, Choi S, Al-Najjar B, Manurung J. Subarnas A, Achmad T, Wardhani S and Wahab H. 2014. Potential Activity of Fevicordin-A from Phaleria macrocarpa (Scheff) Boerl. Seeds as Estrogen Receptor Antagonist Based on Cytotoxicity and Molecular Modelling Studies. *Int. J. Mol. Sci*., **15(5)**: 7225–7249. https://doi.org/10.3390/ijms15057225.

Muttaqin F Z. 2019. Study of molecular docking, molecular dynamic, and toxicity prediction of naphthyridine alkaloid derivatives as protein casein kinase 2-α inhibitor in leukemic cancer. *Pharmacoscript*., **2(1)**: 49–64. https://doi.org/10.36423/pharmacoscript.v2i1.241.

Pires D E, Blundell T L and Ascher D B. 2015. pkCSM: predicting small-molecule pharmacokinetic and toxicity properties using graph-based signatures. *J. Med. Chem*., **58(9)**: 4066–4072.

Pratami M P, Fendiyanto M H, Satrio R D, Nikmah I A, Awwanah M, Farah N, Sari N I P and Nurhadiyanta, N., 2022. In-silico Genome Editing Identification and Functional Protein Change of Chlamydomonas reinhardtii Acetyl-CoA Carboxylase (CrACCase). *Jordan J. Biol. Sci*., **15(3)**: 431–440. https://doi.org/10.54319/jjbs/150312.

Riskesdas K. 2018. Key Results of Basic Health Research (RISKESDAS). *J. Phys. Math. Theor*., **44(8)**: 1–200. https://doi.org/10.1088/1751-8113/44/8/085201.

Ruswanto R, Mardianingrum R, Nofianti T, Fizriani R and Siswandono S. 2023. Computational Study of Bis-(1-(Benzoyl)-3-Methyl Thiourea) Platinum (II) Complex Derivatives as Anticancer Candidates. *Adv. Appl. Bioinforma. Chem*., Volume **16(2023)**: 15–36. https://doi.org/10.2147/AABC.S392068.

Ruswanto R, Mardianingrum R, Siswandono S and Kesuma D. 2020. Reverse Docking, Molecular Docking, Absorption, Distribution, and Toxicity Prediction of Artemisinin as an Anti-diabetic Candidate. *Molekul*., **15(2)**: 88. https://doi.org/10.20884/1.jm.2020.15.2.579.

Sanora G D, Mastura E Y, Handoyo M O M and Purnama E R. 2019. Identification of Anticancer Active Compound from GC-MS Test Results of Zodia Leaves (Evodia suaveolens) Ethanol Extract. *J. Biota*., **5(2)**: 89–95. https://doi.org/10.19109/Biota.v5i2.3374.

Shiau A K, Barstad D, Loria P M, Cheng L, Kushner P J, Agard D A and Greene G L. 1998. The Structural Basis of Estrogen Receptor/Coactivator Recognition and the Antagonism of This Interaction by Tamoxifen. *Cell.*, **95(7)**: 927–937. https://doi.org/10.1016/S0092-8674(00)81717-1

Siswandono. 2020**. Medicinal Chemistry I (Kimia Medisinal I)**, second ed. Airlangga Press, Surabaya.

Tripathi A, Shrinet K, Singh V K and Kumar A. 2019. Molecular modelling and docking of Mus musculus HMGB1 inflammatory protein with CGA. *Bioinformation*., **15(7)**: 456–466. https://doi.org/10.6026/97320630015456.

World Health Organization. 2020. **World case report: cancer research for cancer development**, IARC, France

.